

O(6)—H(6) and O(4)···H(6) distances 1.00 and 1.86 Å with the O(4)···H(6)—O(6) angle 160° are normal. Although the participation of O(4) in the hydrogen bond appears to preserve the symmetry of the exocyclic angles at C(15), O(4) is forced +0.96 (3) Å from the plane of ring *B* with C(19) of the attached methyl group +1.143 (6) Å from the plane. The shortest intermolecular approaches (Table 5) indicate that along [100] and [001] the molecules are held together by van der Waals interactions only.

We thank Professor A. J. Birch of the Australian National University who provided the crystals.

References

- CHATTERJEA, J. N., ROBINSON, R. & TOMLINSON, M. L. (1974). *Tetrahedron*, **30**, 507–512.
- CHEVREUL, M. E. (1808). *Ann. Chim.* **66**, 225–265.
- CHEVREUL, M. E. (1810). *Ann. Chim. Phys.* **82**, 53–85, 126–147.
- CRAIG, J. C., NAIK, A. R., PRATT, R., JOHNSON, E. & BHACCA, N. S. (1965). *J. Org. Chem.* **30**, 1573–1576.
- CROMER, D. T. & LIBERMAN, D. (1970). *J. Chem. Phys.* **53**, 1891–1898.
- CROMER, D. T. & MANN, J. B. (1968). *Acta Cryst.* **A24**, 321–324.
- ISAACS, N. L. & MACKAY, M. F. (1976). *Tetrahedron Lett.* pp. 1921–1922.
- JOHNSON, C. K. (1965). *ORTEP*. Report ORNL-3794. Oak Ridge National Laboratory, Tennessee.
- KARLE, I. L. & KARLE, J. (1966). *Acta Cryst.* **21**, 849–859.
- KARLE, J., HAUPTMAN, H. & CHRIST, C. L. (1958). *Acta Cryst.* **11**, 757–761.
- LUHAN, P. A. & MCPHAIL, A. T. (1972). *J. Chem. Soc. Perkin Trans. 2*, pp. 2006–2010.
- MACKAY, M. F. & ISAACS, N. W. (1980). *Tetrahedron*. In the press.
- MORSINGH, F. & ROBINSON, R. (1970). *Tetrahedron*, **26**, 281–289.
- PERKIN, W. H. & ROBINSON, R. (1907). *J. Chem. Soc.* pp. 1073–1103.
- ROBINSON, R. (1958). *Bull. Soc. Chim. Fr.* pp. 125–134.
- ROBINSON, R. (1977). In *Rodd's Chemistry of Carbon Compounds*, Vol. IV, part E, edited by S. COFFEY, Ch. 22. New York: Elsevier.
- SHELDRICK, G. M. (1976). *SHELX76. Program for Crystal Structure Determination*, Univ. Chemistry Laboratory, Cambridge Univ., England.
- STEWART, R. F., DAVIDSON, E. R. & SIMPSON, W. T. (1965). *J. Chem. Phys.* **42**, 3175–3187.
- WESTIN, L. (1972). *Acta Chem. Scand.* **26**, 2305–2314.

Acta Cryst. (1980). B36, 1610–1615

Electron-Density Distribution in Urea. A Multipolar Expansion

BY D. MULLEN

*Fachrichtung 17.3 Kristallographie, Universität des Saarlandes, D-6600 Saarbrücken,
Federal Republic of Germany*

(Received 7 December 1979; accepted 18 February 1980)

Abstract

A multipole deformation density refinement for urea is presented. Deformation-density maps (model maps) so obtained are compared with a pseudo-atom model, as well as with theoretically calculated densities. An analysis is made of errors arising from attributing phases from $F_{c,n}$ to the observed structure amplitudes.

Introduction

The electron-density distribution in urea has been reported in a previous paper (Scheringer, Mullen, Hellner, Hase, Schulte & Schweig, 1978), in which a pseudo-atom model of the valence density was refined.

A multipolar expansion of the valence density (Hirshfeld, 1971) has now been carried out and a comparison will be made between the two models and also with the theoretical densities described by Scheringer *et al.* (1978).

The same X-ray data set (at 123 K) has been used for all refinements.

Multipole refinement

(a) Description of the model

The expansion of the charge density in the stationary molecule is described by Hirshfeld (1971). The charge density (ρ_{mol}) is expressed in terms of the spherical-

atom density (ρ_a^{at}) with the deformation density (*i.e.* the departures from the spherical-atom distribution) accounted for by a linear combination of localized atomic deformation functions, $\rho_{a,l}$, centred on the atomic nuclei. The total static density is thus the sum of these two contributions for all atoms in the molecule:

$$\rho_a = \rho_a^{\text{at}} + \sum_l c_{a,l} \rho_{a,l}$$

$$\rho_{\text{mol}} = \sum_a \rho_a$$

where the coefficients $c_{a,l}$ are variable population parameters in the least-squares refinement. The atomic deformation functions are described by Hirshfeld (1971). They have the general form

$$\rho_{a,l}(\mathbf{r}) = N_n r^n \exp(-\alpha r_a) \cos^n \theta_k,$$

where r_a is the distance from the atomic centre, θ_k is the angle between the radius vector \mathbf{r}_a and a polar axis \mathbf{k} , n is an integer between 0 and 4, and α is a parameter governing the radial distribution of the deformation functions on each type of atom (variable in the least-squares refinement).

There is a possible total of 35 deformation functions per atom, but this is reduced by symmetry requirements, where some vanish and some are constrained to be equal to others.

(b) Refinement of the urea data

X-ray data for urea at 123 K were measured by Mullen & Hellner (1978) on a Philips PW 1100 automatic diffractometer with graphite-monochromated Mo $K\alpha$ radiation. 288 reflections were obtained out to $\sin \theta/\lambda \leq 0.9 \text{ \AA}^{-1}$, and five of these had $F < 2\sigma(F)$ and were designated as unobserved.

The deformation refinements were carried out up to the quadrupole ($n=2$), octopole ($n=3$) and hexadecapole ($n=4$) levels for C, N and O. Deformation functions centred on C and O have mm and on N atoms m point symmetry. For the H atoms, rotational symmetry was assumed with deformation functions up to $n=2$. A modified f curve for H was used (Hirshfeld, 1977) to account for the contraction of bonded H atoms. The effective nuclear charge was taken as $\zeta = 1.1$ in the expressions for f_{H} (Hirshfeld, 1977).

The possibility of imposing the molecular symmetry plane on the NH_2 group was tested. The numbers of deformation functions and R 's for the various refinements are given in Table 1.

In this paper, the term quadrupole implies the use of all functions up to and including the $n=2$ level, octopole up to and including $n=3$, *etc.* (*e.g.* $n=3$ includes monopoles, dipoles, quadrupoles and octopoles).

The starting parameters for the C, N and O nuclei

Table 1. Agreement factors for the various refinements

	Quadrupole	Octopole	Hexadecapole
Number of deformation functions	25	37	58
R (%)	1.802	1.158	1.063
R_w (%)	1.727	1.081	0.993
Goodness of fit*	1.76	1.13	1.09
$F(000)^\dagger$	62.65	64.03	64.05

* Defined as $[\sum w(|F_o| - |F_c|)^2 / (NO - NV)]^{1/2}$.

† Ideal value = 64.00.

came from a refinement of high-order X-ray data ($\sin \theta/\lambda > 0.6 \text{ \AA}^{-1}$) and those for H from limited neutron data. In the initial stages of the refinement the atomic parameters and the α 's were kept fixed at the starting values and only the deformation coefficients ($c_{a,l}$) were refined. In later stages the α parameters were included and finally all parameters (atomic + deformation) were refined. The atomic parameters of the H atoms, however, were kept fixed at their initial values and were not refined.

Discussion

(a) Results of multiple refinements

The $F_o - F_c$ maps (Fig. 1*a-c*) for the octopole and hexadecapole refinements are reasonably featureless, with the highest residual peaks [in N-H(2)] of the order of 0.1 e \AA^{-3} . In contrast, the quadrupole refinement shows peaks in all bonds which are greater than 0.1 e \AA^{-3} and in the N-H(2) bond a peak of 0.2 e \AA^{-3} . A deep hole (-0.26 e \AA^{-3}) occurs near the C atom.

Agreement factors for all three refinements are summarized in Table 1. R for the octopole (1.158%) and quadrupole (1.802%) refinements are significantly different according to the Hamilton (1965) test at the 0.005 level. The hexadecapole refinement ($R = 1.063\%$), on the other hand, does not represent

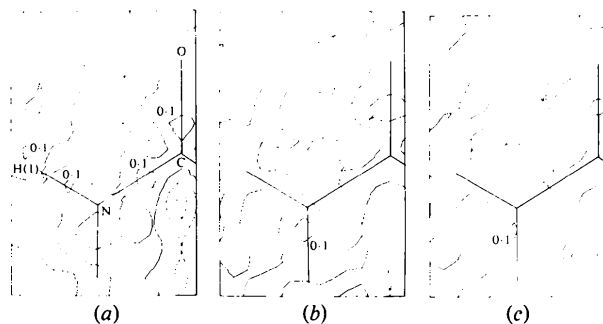


Fig. 1. ($F_o - F_c$) maps for (a) quadrupole, (b) octopole and (c) hexadecapole refinements. Contour intervals are 0.1 e \AA^{-3} . Zero and positive contours solid lines, negative contours dashed.

a significant improvement over the octopole with the same criteria. These conclusions are substantiated by the goodness-of-fit values and calculated $F(000)$ values which are near-ideal in both octopole and hexadecapole refinements (Table 1).

Normal-probability plots (Fig. 2) of the differences ΔF show straight lines with unit slope for both octopole and hexadecapole refinements but not for the quadrupole refinement, supporting the conclusions of the R -factor analysis above.

By imposing a mirror plane on the NH_2 group (*i.e.* with mm point symmetry) we increase the agreement factors to $R = 1.271\%$, $R_w = 1.177\%$ and the goodness-of-fit to 1.22 for the octopole refinement. The total number of deformation parameters is reduced to 32. This increase in R is significant at the 0.005 level (Hamilton, 1965), indicating that the two N—H bonds are not identical under the criteria indicated. From the normal-probability plots of ΔF , however, no distinction is evident, so that the difference is marginal.

Significant differences were found between core parameters of the quadrupole and octopole refinements, in particular for $N_{x,y}$, where the difference is about 3.8σ . Other parameter differences lie between 1 and 2σ . The hexadecapole and octopole refinements, in contrast, show differences which are not much greater than 1σ . Table 2 gives atomic parameters from the octopole refinement.

The scale factors from the octopole and hexadecapole refinements differ by only 0.35%, whereas that of the quadrupole refinement is 1.24% smaller than that of the octopole refinement. (Scale factor multiplies F_c .)

The same trends are observed in the deformation parameters, where the largest differences occur between the quadrupole and the other two models. The α 's for the latter two refinements agree within about 1σ , whereas the quadrupole refinement shows differences up to 3.8σ [for $\alpha(\text{N})$].

Of the additional 21 hexadecapole parameters, nine refined to values greater than 1σ , but all these were less than 2σ .

Dynamic and static deformation-density maps (model maps) are given in Figs. 3(a)–(c) and 4(a)–(c)

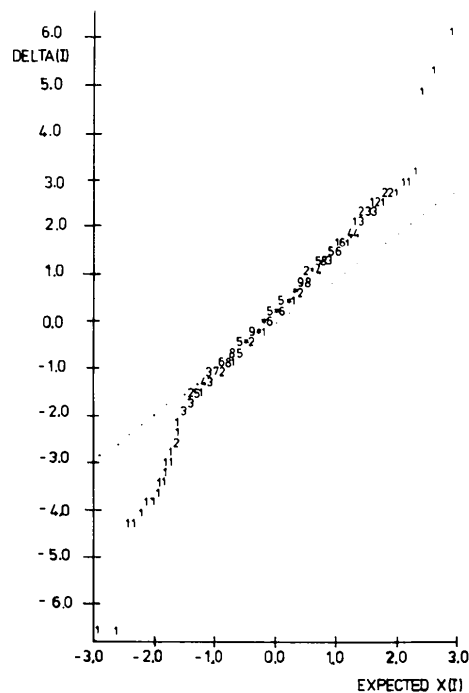
Table 2. Atomic parameters from the octopole refinement (U_{ij} are $\times 10^4$)

$$y = \frac{1}{2} + x; U_{22} = U_{11}; U_{23} = U_{13}.$$

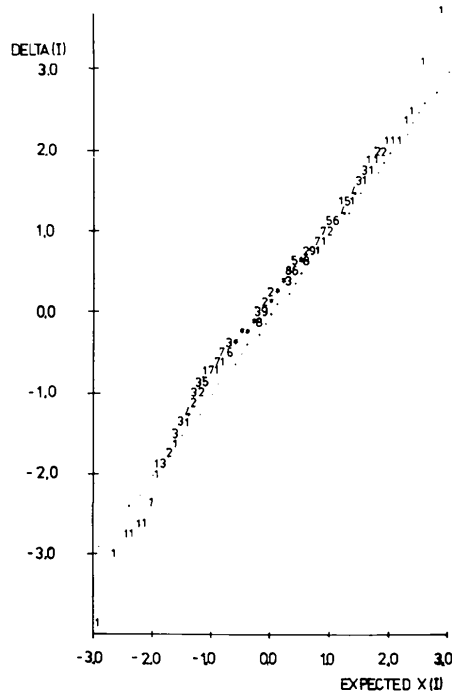
$$T = \exp[-2\pi^2(U_{11}h^2a^{*2} + U_{22}k^2b^{*2} + U_{33}l^2c^{*2} + U_{12}hka^*b^* + U_{13}hla^*c^* + U_{23}klb^*c^*)].$$

	x	z	U_{11}	U_{33}	U_{12}	U_{13}
C	0	0.3282 (2)	130 (2)	55 (2)	-5 (3)	0
O	0	0.5962 (4)	167 (2)	62 (4)	13 (4)	0
N	0.14504 (9)	0.1784 (1)	253 (2)	81 (1)	-140 (2)	1 (1)
H(1)	0.2561	0.2811	410	246	-206	-30
H(2)	0.1429	-0.0383	406	188	-154	12

respectively. The e.s.d.'s of the maps are 0.043, 0.025 and 0.023 $\text{e} \text{ \AA}^{-3}$ for the quadrupole, octopole and hexadecapole refinements, respectively. Peak heights for all three refinements are summarized in Table 3(a)



(a)



(b)

Fig. 2. Normal-probability plots (Abrahams & Keve, 1971) for (a) quadrupole and (b) octopole refinements. Numbers indicate number of values at a particular point. Asterisks indicate more than 10 points.

for the dynamic maps and in Table 3(b) for the static maps. An examination of Table 3(a) shows that the octopole and hexadecapole maps have a maximum difference in the O lone-pair peak of $0.04 \text{ e } \text{Å}^{-3}$. This is less than 2σ .

In contrast, the quadrupole model has a peak of only $0.06 \text{ e } \text{Å}^{-3}$ in the C—O bond and a C—N peak situated very close to the N core.

(b) Comparison with pseudo-atom model

In a previous study of the density distribution in urea (Scheringer *et al.*, 1978) with the same data set, a

Table 3. Peak heights from various refinements ($\text{e } \text{Å}^{-3}$)

	Quadrupole	Octopole	Hexadecapole
(a) Dynamic densities			
C=O	0.06	0.29	0.32
C—N	0.67	0.52	0.51
N—H(1)	0.29	0.28	0.30
N—H(2)	0.29	0.25	0.26
O (lone pair)	0.62	0.56	0.60
(b) Static densities			
C=O	0.09	0.40	0.45
C—N	0.92	0.61	0.58
N—H(1)	0.70	0.47	0.52
N—H(2)	0.68	0.43	0.41
O (lone pair)	0.80	0.75	0.67

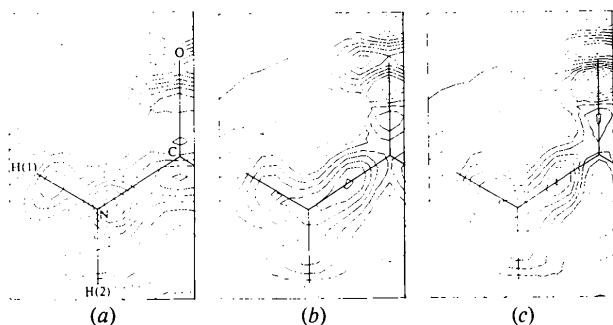


Fig. 3. Dynamic deformation densities for (a) quadrupole, (b) octopole and (c) hexadecapole refinements. Contours as for Fig. 1.

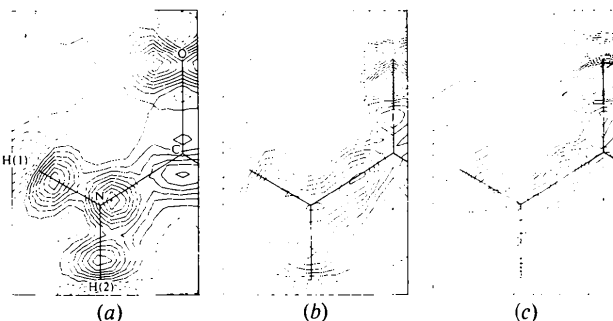


Fig. 4. Static deformation densities for (a) quadrupole, (b) octopole and (c) hexadecapole refinements. Contours as for Fig. 1.

pseudo-atom model of the valence density was tested. Ellipsoidal charge clouds were placed in the bonds to represent the bonding density. The core parameters from this pseudo-atom refinement (Mullen & Hellner, 1978) show good agreement (for C, N and O) with the octopole parameters, the biggest difference being 2.1σ for N(z). Differences with the quadrupole model are at a maximum for the positional parameters of N (*i.e.* $\sim 4\sigma$).

An examination of the deformation-density maps, however, shows that the pseudo-atom model results in a map most closely resembling the quadrupole refinement. The most prominent feature is the failure of both the pseudo-atom model and the quadrupole model to produce the polarity of the C=O bond with a negative peak near O (*cf.* octopole and hexadecapole maps). The C=O bond peak in the static density map is only $0.12 \text{ e } \text{Å}^{-3}$ (Scheringer *et al.*, 1978) compared with $0.09 \text{ e } \text{Å}^{-3}$ in the quadrupole map and $0.40 \text{ e } \text{Å}^{-3}$ in the octopole map. The C—N peak is close to the N core in both the former maps, but is in the bond centre in the octopole map.

R for the pseudo-atom model (1.6%) is close to the quadrupole refinement (1.8%) but much higher than the octopole value (1.1%) although 34 subsidiary parameters were used in the pseudo-atom model (*cf.* 37 for the octopole refinement).

(c) Comparison with theoretical deformation densities

Theoretical static and dynamic deformation densities for urea, calculated with a 4-31G basis set, are given by Scheringer *et al.* (1978). These maps also show a polar C—O bond in agreement with the octopole and hexadecapole models. Comparing the static densities, we find that the C—O bond peak ($0.51 \text{ e } \text{Å}^{-3}$) and N—H peak ($0.55 \text{ e } \text{Å}^{-3}$) are in reasonable agreement with those of the octopole and hexadecapole refinements. The C—N peak ($0.34 \text{ e } \text{Å}^{-3}$) is considerably lower and the lone-pair peak on O ($1.2 \text{ e } \text{Å}^{-3}$) is much higher than the corresponding values from the multipole refinements.

The negative peak in the C—O bond near O with a value of about $-0.5 \text{ e } \text{Å}^{-3}$ in the theoretical dynamic density is in good agreement with the corresponding hexadecapole value ($-0.5 \text{ e } \text{Å}^{-3}$) but somewhat deeper than the octopole value ($-0.3 \text{ e } \text{Å}^{-3}$).

The location and shape of the lone-pair peaks on O deserve closer attention. In the octopole map, the peaks are comparable in these respects to the theoretical maps. These peaks in the quadrupole and pseudo-atom maps are not only of a different shape compared with the octopole map (Scheringer *et al.*, 1978), but in the quadrupole map they are shifted into the C—O bond (Fig. 3a).

In the hexadecapole map the two related residual peaks on O are no longer resolved but form a single

broad peak (Fig. 3c). The additional hexadecapole functions on O are all of the order of 1σ or less and are not responsible for this marked change in the lone-pair shape. In comparison, N and C have fourth-order functions of greater significance. The z parameter of O, however, shows a shift of 0.004 \AA towards C on going from the octopole to the hexadecapole model. Although this shift is less than 1σ , it is enough to cause the difference in peak shape found. Deformation maps are thus very sensitive even to small changes in atomic positions, especially for features (such as lone-pair residual peaks) close to the nuclei.

(d) Phase differences for $F_{o,x}$ and $F_{c,N}$

The magnitude of the mean phase differences $|\overline{\Delta\phi}|$ between $F_{o,x}$ and $F_{c,N}$ for the different $|F|$ and $\sin \theta/\lambda$ ranges are given in Table 4(a,b) and Fig. 5(a,b). $F_{o,x}$ represents (in the present case) the structure factors obtained from the multipole refinement and $F_{c,N}$ those calculated on the basis of a spherical-atom model with the same atomic parameters as the multipole model. The multipole model is assumed to yield the correct phases for the observed structure amplitudes and $\Delta\phi$ then represents errors arising through attributing phases from a spherical-atom model to the observed F 's. These errors, which are reflected in the electron-density maps so calculated, have been discussed by Mullen & Scheringer (1978) and by Thomas (1978).

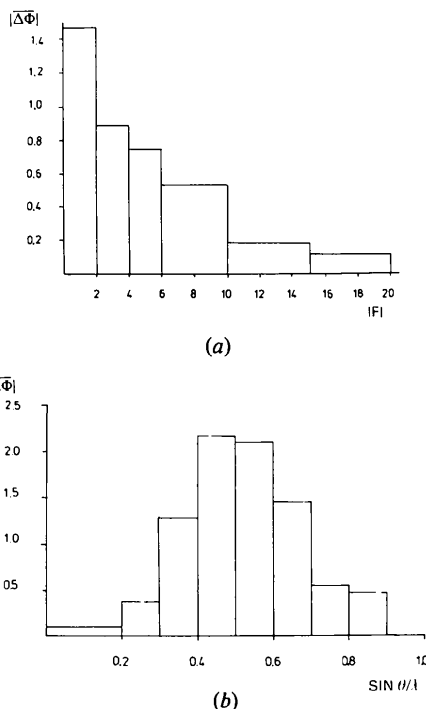


Fig. 5. Variation of $|\overline{\Delta\phi}|$ ($^\circ$) with (a) $|F|$ and (b) $\sin \theta/\lambda$.

Table 4. Mean phase differences between $F_{o,x}$ and $F_{c,N}$ ($^\circ$)

(a) Variation with $ F $		(b) Variation with $\sin \theta/\lambda$	
$ F $ ranges	$ \overline{\Delta\phi} $	$\sin \theta/\lambda$ ranges	$ \overline{\Delta\phi} $
0-2	1.47	0.0-0.2 \AA^{-1}	0.09
2-4	0.89	0.2-0.3	0.37
4-6	0.75	0.3-0.4	1.26
6-10	0.53	0.4-0.5	2.16
10-15	0.18	0.5-0.6	2.10
15-20	0.12	0.6-0.7	1.44
		0.7-0.8	0.54
		0.8-0.9	0.46

Table 4(a) and Fig. 5(a) show the variation of $|\overline{\Delta\phi}|$ for ranges of $|F|$. The $|\overline{\Delta\phi}|$ values decrease with increasing $|F|$ in agreement with the trend found by Thomas (1978), the values lying between 0.12 and 1.47° for urea and between 0.66 and 1.79° for lithium formate monohydrate.

Table 4(b) and Fig. 5(b) give the variation of $|\overline{\Delta\phi}|$ for $\sin \theta/\lambda$ ranges. $|\overline{\Delta\phi}|$ values are highest between 0.3 and 0.7 \AA^{-1} in $\sin \theta/\lambda$ (1.26 – 2.16°) and decrease to about 0.5° at 0.9 \AA^{-1} in $\sin \theta/\lambda$. This can be understood in terms of the fall-off of the contribution from valence electrons in the high-angle region, so that a spherical-atom model represents a better approximation to the phases for the experimental structure factors in this region of $\sin \theta/\lambda$ than in lower regions. Lundgren (1979) also points out that the deformation functions give little contribution to the high-order data ($\sin \theta/\lambda > 0.7 \text{ \AA}^{-1}$).

As $\sin \theta/\lambda$ decreases from about 0.5 \AA^{-1} , the $|\overline{\Delta\phi}|$ values also decrease rapidly, reaching a value of only 0.09° in the range 0 – 0.2 \AA^{-1} . For $F(000)$ (*i.e.* at $\sin \theta/\lambda = 0$), the $\Delta\phi$ value must be 0 , so that a fall-off with decreasing reciprocal path length is understandable.

Summary

The multipole refinement must be carried out with deformation functions up to the order $n = 3$ (*i.e.* octopole level) in order to obtain an adequate description of the density distribution in the molecule. Lower-order refinements (quadrupole level) are insufficient. Higher-order refinements (*i.e.* hexadecapole level) result in a large increase in refinable parameters and introduce relatively minor changes in the deformation density. At least for first-row elements such as C, O and N, hexadecapoles appear to be largely superfluous. However, the effect on the shape of the lone pair on O should be noted.

Both the quadrupole and the pseudo-atom model fail to describe the density in the C–O bond properly with the occurrence of a hole (negative peak) near O. Comparison with theoretically calculated densities

shows large discrepancies for the C–N bond and O lone-pair densities.

The mean phase differences $|\overline{\Delta\varphi}|$ between $F_{o,x}$ and $F_{c,N}$ vary with $|F|$ more sharply than was found by Thomas (1978) for lithium formate monohydrate. For urea, the maximum value of 1.47° occurs for low $|F|$ values and $|\overline{\Delta\varphi}|$ decreases with increasing $|F|$. With $\sin \theta/\lambda$, $|\overline{\Delta\varphi}|$ has a peak at about 0.5 \AA^{-1} and falls off at lower and higher angles.

Thomas (1978) has compared (X–N) and deformation refinement procedures and discussed the advantages of the latter, particularly for non-centrosymmetric cases, in terms of the problem of phases discussed above.

The author thanks Klaus Eichhorn for helpful discussions, especially concerning the use of the

multipole refinement program in its version adapted to the TR 440 computer at Saarbrücken.

References

- ABRAHAMS, S. C. & KEVE, E. T. (1971). *Acta Cryst.* **A27**, 157–165.
 HAMILTON, W. C. (1965). *Acta Cryst.* **18**, 502–510.
 HIRSHFELD, F. L. (1971). *Acta Cryst.* **B27**, 769–781.
 HIRSHFELD, F. L. (1977). *Isr. J. Chem.* **16**, 226–229.
 LUNDGREN, J. O. (1979). *Acta Cryst.* **B35**, 1027–1033.
 MULLEN, D. & HELLNER, E. (1978). *Acta Cryst.* **B34**, 1624–1627.
 MULLEN, D. & SCHERINGER, C. (1978). *Acta Cryst.* **A34**, 476–477.
 SCHERINGER, C., MULLEN, D., HELLNER, E., HASE, H. L., SCHULTE, K.-W. & SCHWEIG, A. (1978). *Acta Cryst.* **B34**, 2241–2243.
 THOMAS, J. O. (1978). *Acta Cryst.* **A34**, 819–823.

Acta Cryst. (1980). **B36**, 1615–1621

Rigid-Body Coordinates of Pyranose Rings

BY B. SHELDRIK AND D. AKRIGG

Astbury Department of Biophysics, University of Leeds, Leeds LS2 9JT, England

(Received 9 January 1980; accepted 18 February 1980)

Abstract

161 published structures containing pyranose rings, listed in the Cambridge Crystallographic Data File, have been investigated to establish the orthogonal coordinates of the average ring. Details are given of the mathematical procedures used in the calculations, of the results for the various hexoses, and of variations found.

Introduction

In crystallographic structural work, it is often advantageous to be able to treat a group of atoms as a rigid body, *i.e.* a group in which the atoms maintain a constant relationship to each other in terms of the distances between the atoms and the angles between interatomic vectors, when the whole group of atoms is rotated about any axis or translated in any direction. Two examples may be given. In the calculation of the overall scattering curve for use with direct methods of crystallographic phase-angle determination, the inclusion of a known rigid group, in terms of a molecular scattering factor, in place of the equivalent number of atomic scattering factors, can improve the

accuracy of the scale-factor determination and the unitary scattering factors and hence produce more reliable phase angles. Secondly, if the number of independent parameters in a structure determination, *e.g.* positional and thermal vibration parameters, is large compared with the number of independent observational parameters, then the introduction of a group of atoms, treated as a rigid body, can be used to reduce the number of structural parameters to be refined. In this case, the $3n$ positional parameters of n atoms are replaced by six parameters for the rigid body consisting of three positional and three rotational parameters.

These advantages require that the specification of the atoms of the rigid group is an accurate representation of the group involved and, though it is usually possible to calculate the dimensions of such a group from known values of bond lengths and angles, other factors may make slight, but significant, differences from the calculated model.

One method of establishing the most accurate representation of a particular group is to examine previously determined structures which contain that group and, from these known conformations, derive the atom parameters which give the best least-squares fit. Care must be taken, however, to ensure that the